

## An Experimental Investigation of A Low Speed Double - Sided Linear Induction Motor

S.A. EL-Drieny

Electrical Engineering Department

Faculty of Engineering

EL-Mansoura University

EL-Mansoura, Egypt.

### Abstract

An experimental study of a four pole, low speed, 21 cm long double-sided linear induction motor (DSLIM) is presented in this paper. Experiments are carried out using a rotary type test facility with flat stator cores and an aluminium rotating disc. Attention is concentrated on the braking of such type of DSLIM, especially when the two stator sides are connected in parallel or in series. The performance testing are reported for both constant current and constant voltage operations. Measurements of the air-gap flux density over the stator length are carried out under both the no-load and braking conditions. The measured results compared in four different cases: single sided stator without back iron, single sided stator with back iron, double-sided stator connected in parallel, and double-sided stator connected in cascade. A phase shift of zero or 120 electrical degrees is taken while testing the last case. The study aims to increase the understanding of the DSLIM behaviour under both load and braking conditions. The results recommend the cascade connection with zero phase shift as the best connection of the DSLIM; due to the high thrust and the low braking time.

### 1. Introduction

In the recent years, considerable interest has developed in the use of linear induction motors in the building of the propulsion for the future high speed trains. The double-sided linear induction motor (DSLIM) provides a simple, rigid structure. Because of the structural advantages, this motor is being considered as a suitable type of propulsion motor for both high speed and low speed trains. However, this application requires a good technique for speed control and electrical braking due to frequent stops. Present information on electrical braking of DSLIM is not sufficient. Therefore, detailed laboratory tests and more theoretical analyses are required. The general aim of this paper is to spot the light on detailed laboratory tests of DSLIM, according to the numerical data given in reference [1], under both the no-load and the braking conditions.

The tests are carried out for the following cases:

- a. Single sided excited stator without back iron.
- b. Single sided excited stator with back unexcited stator.
- c. Double-sided excited stators with parallel connection.
- d. Double-sided excited stators with cascade connection, with phase shift zero electrical degree.
- e. Double-sided excited stators with cascade connection, with phase shift 120 electrical degrees.

## 2. Description of Motor Model

A laboratory motor model was constructed to enable the detailed experimental studies. The model consists of two parts: a double-sided stator as the primary part and an aluminium rotating disc as the secondary part. The disc is of 7 mm thickness and fixed on an axis which is free to rotate between two bearings. Each stator side is wound for four poles and fitted in flat, 21 cm long, laminated core. Both stator-sides are symmetrically mounted around the aluminium disc. The motor was fed from 3-phase 50 Hz constant current supply ( 3 Amperes ) or constant voltage supply ( 30 Volts ). Either of the constant current source or the constant voltage source is obtained by three adjustable single phase transformers.

Each stator is mounted in a rigid yoke assembly, and supported to a trapezoidal mild steel frame through two aluminium pieces; to minimize the magnetic leakage from the stator core to the frame. The centre line of each stator is at a radius of 21 cm from the disc axis. Each stator consists of 5 cm stack of 0.35 mm silicon steel laminations with an inorganic inter-laminar coating. These laminations are supported together with two mild steel plates of 5 mm thick, one at each side. Twelve open slots are cut by a milling machine into the face of the assembled core. Each slot has 1.5 cm depth, 1.25 cm width. The windings are single layer with one slot per pole per phase, and 150 turns per coil.

The facility of adjusting the air-gap length had been considered. It is taken to be 14 mm between the two stators sides inclusive the thickness of an aluminium disc.

The rotor disc diameter is chosen to be large compared with the stator width. Accordingly the peripheral speed of the disc is determined by the disc periphery tangential to the stator centre line.

The synchronous speed is 5.3 m / sec. at the centre of the stator, which corresponds to a pole pitch of 5.3 cm. Low synchronous speed results in low efficiency but it is desirable for the laboratory measurements.

Supplementary cooling is provided for all parts of the motor model by directing the cooling air at the trailing edge of the disc.

## 3. Experimental Results

### 3.1 Magnetic Flux Density Distribution Along The Stator Surface.

To measure the flux density along the stator core, a search coil consists of 5 turns is wound and it is fixed at the top of each tooth. A voltage proportional to the flux density is induced, and it can be measured at the search coil terminals across an oscilloscope.

Figures (1-a), (1-b), (1-c), (1-d), and (1-e) show the flux density along the stator surface at zero slip. The figures (2-a), (2-b), (2-c), (2-d), and (2-e) show the flux density along the stator surface at unity slip. It will be noticed from the figures that the flux density is weakened at the entry-end due to the entry-end effects [ 2,3,4 ] then it is built up gradually. There are dips and sharp rises, due to the discrete distribution of the amper-turns in the slots and the reflected exit-end wave.

The flux density in case of single sided stator backed by the other stator part, unexcited, is greater than the flux density in case of single sided without back iron due to the reduction of the magnetic reluctance. The amplitude of the flux density in case of the double-sided cascade connection with zero phase shift is greater than that the double-sided parallel connection. In case of the cascade connection with 120 electrical degrees phase shift, the flux density is too small.

### 3.2 Thrust

Measurements of the thrust is carried out by using a calibrated spring on one side of an attached wheel to the axle of the disc rotor and balanced with weights on the other side of the wheel.

Figure (j) shows the measured thrust per meter under constant current and constant voltage operations. It follows now some comments about the maximum values of the measured thrust, which are also given in Table I

#### 3.2.1 Under constant current operation :

- The maximum thrust developed in case of double sided cascade connection with zero phase shift is greater than that developed in case of double sided parallel connection by about 1.95 times.
- The maximum thrust developed in case of double sided parallel connection is greater than developed in case of single sided excited stator, backed by unexcited stator, by about 1.2 times.
- The maximum thrust developed in case of single sided excited stator backed by unexcited stator is greater than that developed in case of single sided excited stator by about 1.45 times.
- The maximum thrust developed in case of double sided cascade connection with zero phase shift is greater than that developed in case of double sided cascade connection with 120 electrical degrees phase shift by 4.13 times.

#### 3.2.2 Under constant voltage operation :

- The maximum thrust developed in case of double sided cascade connection with phase shift zero is greater than that developed in case of double sided parallel connection by 1.67 times approximately.
- The maximum thrust developed in case of double sided parallel connection is greater than that developed by single sided backed by unexcited stator by 1.45 times.
- The maximum thrust developed in case of single sided backed by unexcited stator is greater than that developed by single sided excited stator by 1.45 times.
- The maximum thrust developed in case of double sided cascade connection with zero phase shift is greater than developed in case of double sided cascade connection with 120 electrical degrees by 3.85 times.

### 3.3 Efficiency

Figure (k) shows the measured efficiency under constant current and constant voltage operations. The following observations can be reported about the maximum values of the efficiency, which are also given in Table I.

#### 3.3.1 Under constant current operation :

- The maximum efficiency in case of double sided cascade connection is greater than that measured in case of the double sided parallel connection by 1.45 times.
- The maximum efficiency in case of double sided parallel connection is greater than that measured in case of single sided, backed by an unexcited stator, by 1.11 times.
- The maximum efficiency in case of single sided backed with an unexcited stator is greater than that obtained in case of single sided excited stator by 2.11 times.
- The maximum efficiency in case of double sided cascade connection with

zero phase shift is greater than that obtained in case of double sided cascade connection with phase shift 120 electrical degrees by about 4.17 times

### 3.3.2 Under constant voltage operation :

- (a) The maximum efficiency in case of double sided with cascade connection is greater than that obtained in case of double sided parallel connection by about 1.32 times
- (b) The maximum efficiency 1.32 in case of double sided parallel connection is greater than that measured in case of single sided backed with an unexcited stator by 1.30 times
- (c) The maximum efficiency in case of single sided backed with an unexcited stator is greater than that obtained in case of single sided excited stator by 2 times.
- (d) The maximum efficiency in case of double sided cascade connection with zero phase shift is greater than that measured in case of double sided with cascade connection with 120 electrical degrees phase shift by about Four times.

Generally, the measurements pointed out that the efficiency is so bad due to the existence of both the entry and exit ends power loss and the large air-gap.

### 3.4 Braking Time

In order to brake the model, the phase sequence had been reversed in any side of the two stators. Figure (5-a) shows the thrust versus the braking time during constant current operation. It is shown from the figure that the developed thrust by the double sided cascade connection with zero phase shift is greater than the braking thrust developed by the double sided with parallel connection by 1.35 times and both of them cause complete braking at the same time.

The figure also shows that the double sided cascade connection with zero phase shift developed braking thrust greater than that developed by the double sided Cascade connection with 120 electrical degrees phase shift by 2.78 times and both of them cause complete braking time at the same time.

Figure (5-b) shows the braking thrust versus the braking time during constant voltage operation. It is shown from the figure that the double sided cascade with phase shift zero develops braking thrust greater than that developed by double sided parallel connection by 1.1 times and both of them cause complete braking at the same time. Also with the double sided cascade connection with zero phase shift develops braking thrust greater than that developed by the double sided cascade connection with 120 electrical degrees phase shift by 2.2 times and both of them cause complete braking at the same time.

### 3.5 Supply currents, in case of voltage operation

Figures (6-a), (6-b), (6-c), (6-d), and (6-e) show the supply current measurements at constant voltage. The measured currents reveal that , the phase winding which is near the entry -end draws more current from the supply than the windings of the phases located farther from the entry-end. Accordingly, more copper losses is expected in this phase, which causes a non-uniform electromagnetic force of the primary windings.

The supply current measurements in case of double sided cascade connection with phase shift 120 electrical degrees is more unbalanced than that for any connection. This may be due to higher unbalanced impedances

The primary currents are almost constant over a wide slip in this DSLIM. But in the ordinary induction motors, the primary currents decrease as the slip approaches zero, and at this slip only the exciting current flows in the primary windings.

### 3.6 Supply voltages, in case of constant current operation

In order to overcome the above mentioned unbalance in the primary electromagnetic force, the constant voltage source is replaced by constant current source. Figures (7-a), (7-b), (7-c), (7-d), and (7-e) show the measured supply voltages. It is shown that the applied supply voltage to the phase winding near the exit-end is greater than that applied to the phase winding near the entry-end.

### 4 Conclusions

The building and testing of double sided linear induction motor DSLIM as a test model have resulted in a deep understanding of the overall behaviour and characteristics of the machine under no load, load and braking conditions. By use of the model, the thrust, efficiency, braking time and the air-gap flux density along the stator have been investigated under constant current and constant voltage operation conditions. The laboratory model is sufficiently flexible to examine the best connection for such type of linear induction motor. This connection is found to be the cascade connection with zero electrical degree phase shift. It develops high braking thrust at the same braking time and gives high normal thrust. These two advantages are essential for practical application.

The results show that the primary currents are almost constant over a wide slip range in the test model. But in the ordinary induction motor, the primary currents decrease as the slip approaches zero, and at this slip only the exciting current flows in the primary windings.

The experimental tests pointed out that high thrust can be obtained under constant current operation than under constant voltage operation. Generally, the efficiency is too bad due to the large air-gap and the existence of the entry and exit ends power loss.

### 5 References

- [1] EL-Drieny S.A. " Effects of some design parameters on the performance of the double-sided linear induction motor " , Bulltin of the Faculty of Engineering EL-Mansoura University ,Vol. 11, No. 1, June 1986, pp.E 69 - E81.
- [2] Iwamoto M. , Sakabe S., Itani K., Kitagawa K., and Utsumi G. "Experimental and theoretical study of high-speed single-sided linear induction motors" IEE. , Proce. Vol 128, No. 6 November 1981.
- [3] Choho O.C. ,Klman G.B., and Robinson J.I."Experimental evaluation of a high-speed double sided linear induction motor ". presented at the IEEE., PES. ,summer meeting of July 1974 for transaction pp 10-17.
- [4] Klman G.B. and Elliott D.G. "Linear induction motor experiments in comparison with mesh/matrix analysis "Presented at the IEEE., PES., winter meeting of Jan. 1974 for transactions pp 1624-1633.

Case of the Test		a	b	c	d	e
maximum Thrust N/m	Constant Current	90	137	175	333	80
	Constant Voltage	80	117	170	300	78
maximum Efficiency %	Constant Current	9	11.7	16.5	27	7.5
	Constant Voltage	7.4	11.7	15	25.5	6

Table I: The maximum thrust and maximum efficiency measured in the different cases of the test.

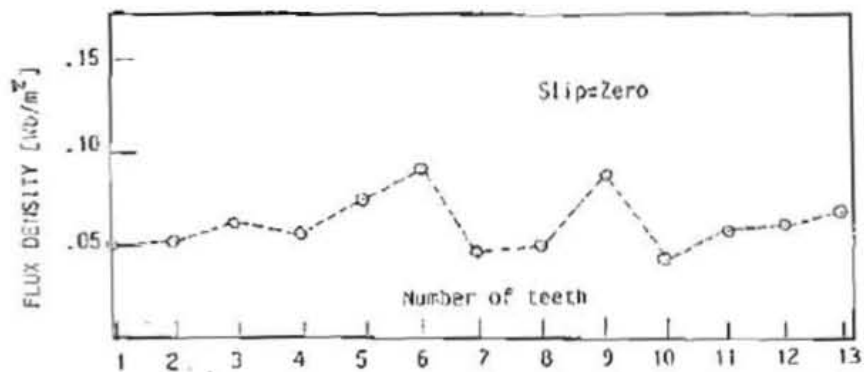


Fig. (1-a) : Measured flux-density-distribution curve, for single sided excited stator

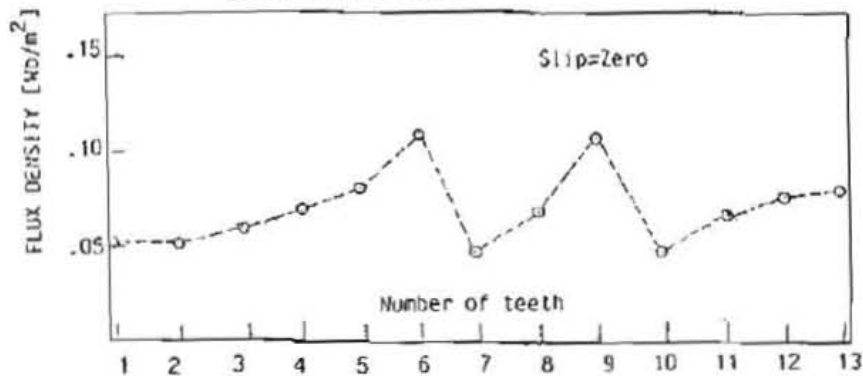


Fig.(1-b) : Measured flux-density-distribution curve, For single sided-excited stator-backed by unexcited stator.

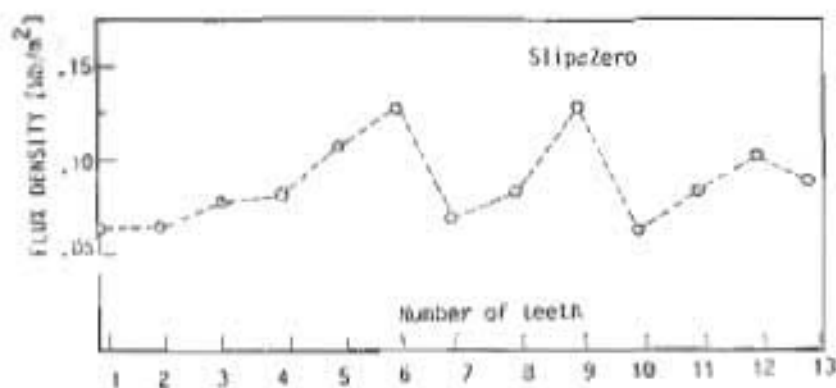


Fig.( i-c ) : Measured flux-density - distribution curve for double sided excited stator - parallel connection.

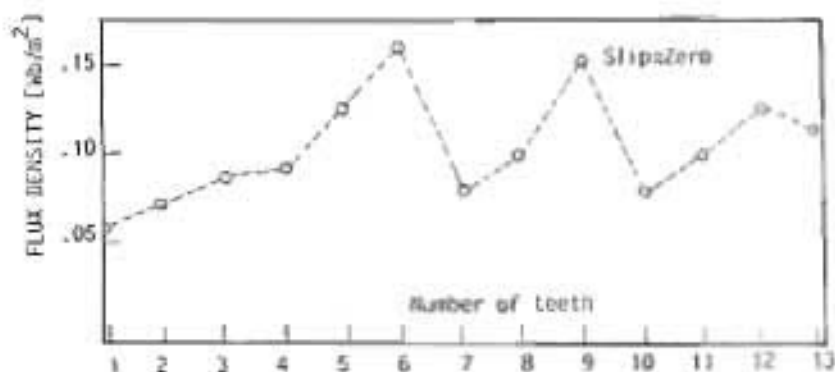


Fig.( i-d ) : Measured flux - density-distribution for double sided, excited stator with zero electric degree phase shift.

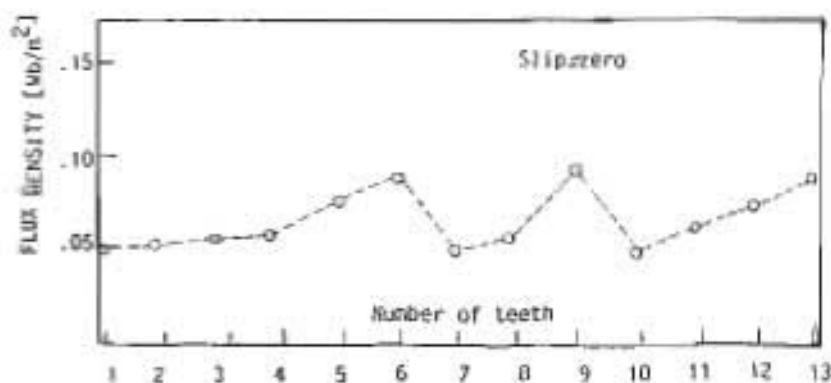


Fig.( i-e ) : Measured flux - density - distribution for double sided excited stator with 120 electric degree phase shift.

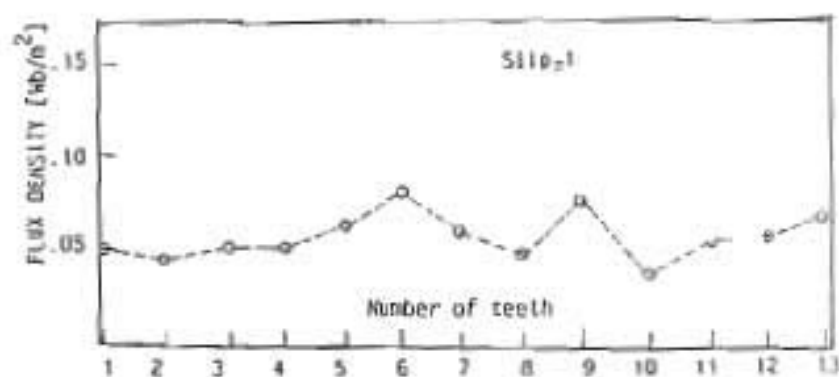


Fig. (2-a) : Measured flux-density-distribution curve for single sided excited stator .

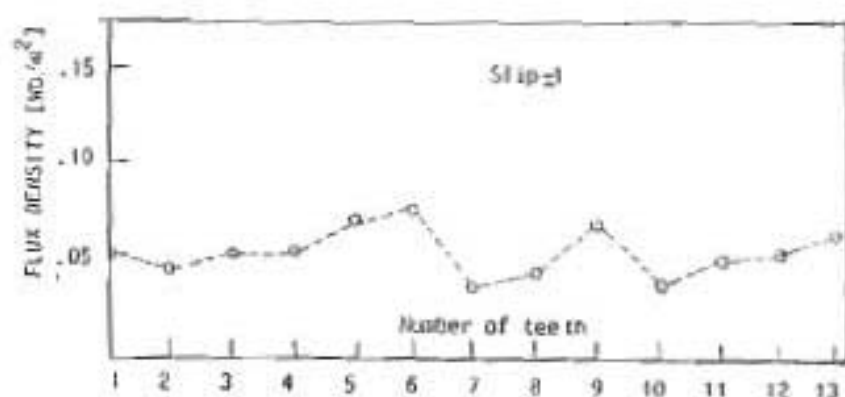


Fig. (2-b) : Measured flux-density-distribution curve for single sided-excited stator backed by unexcited stator .

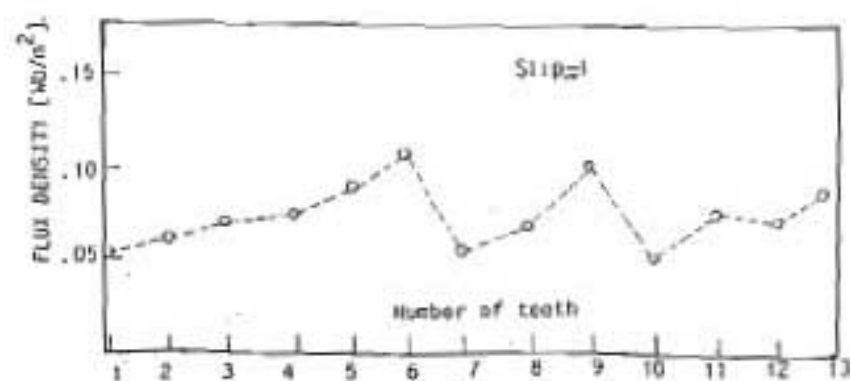


Fig. (2-c) : Measured flux-density-distribution curve for double sided excited stator-parallel connection .



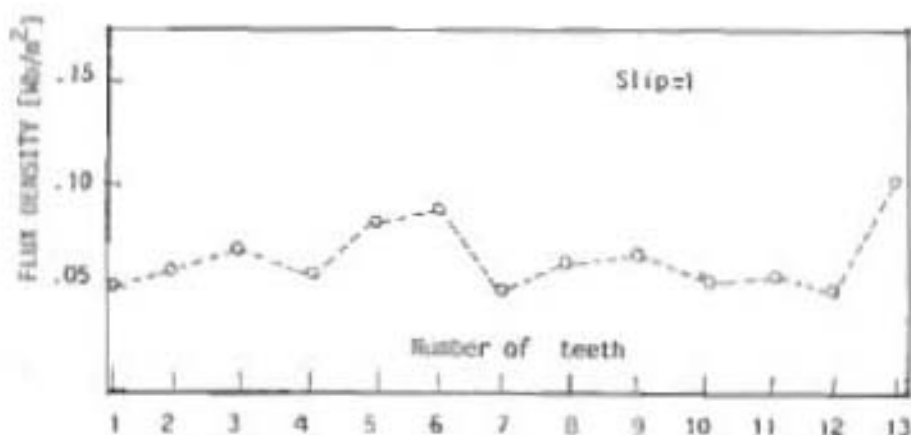


Fig.(2-d) : Measured flux - density-distribution for double sided excited stator with zero electric degree phase shift.

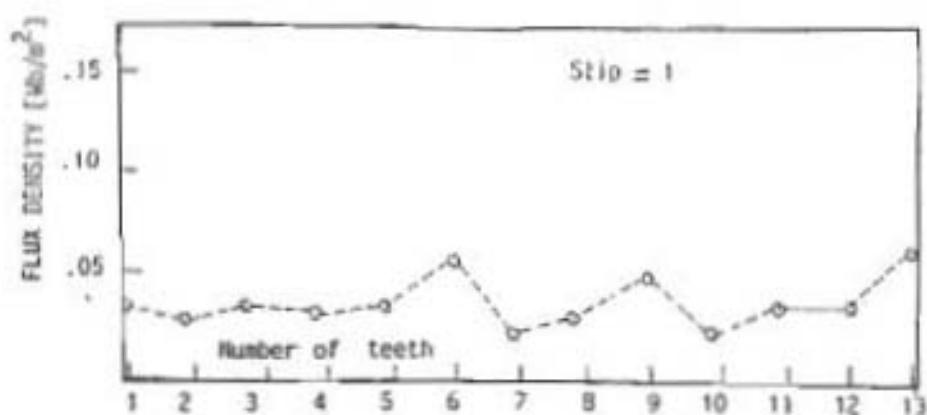
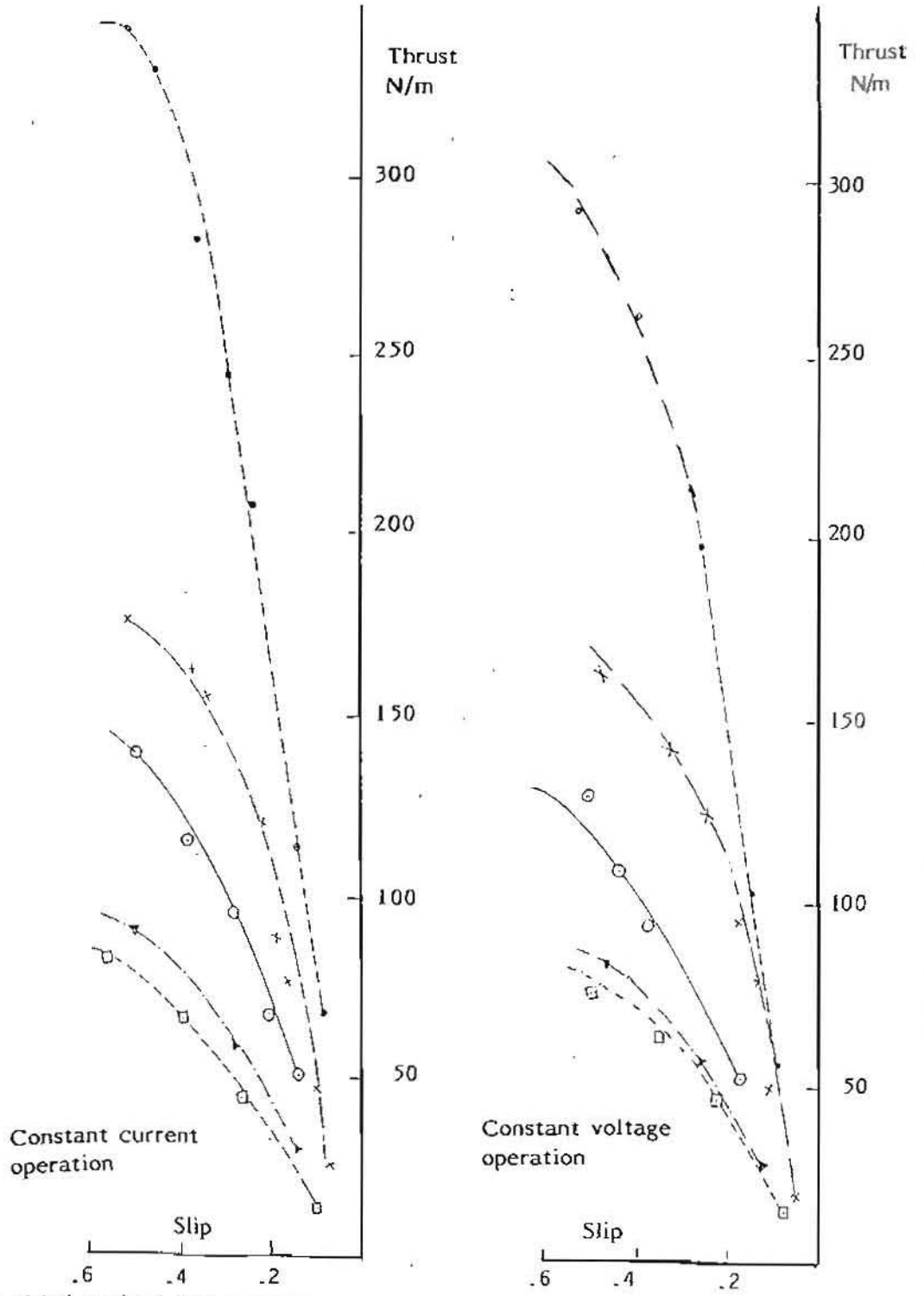
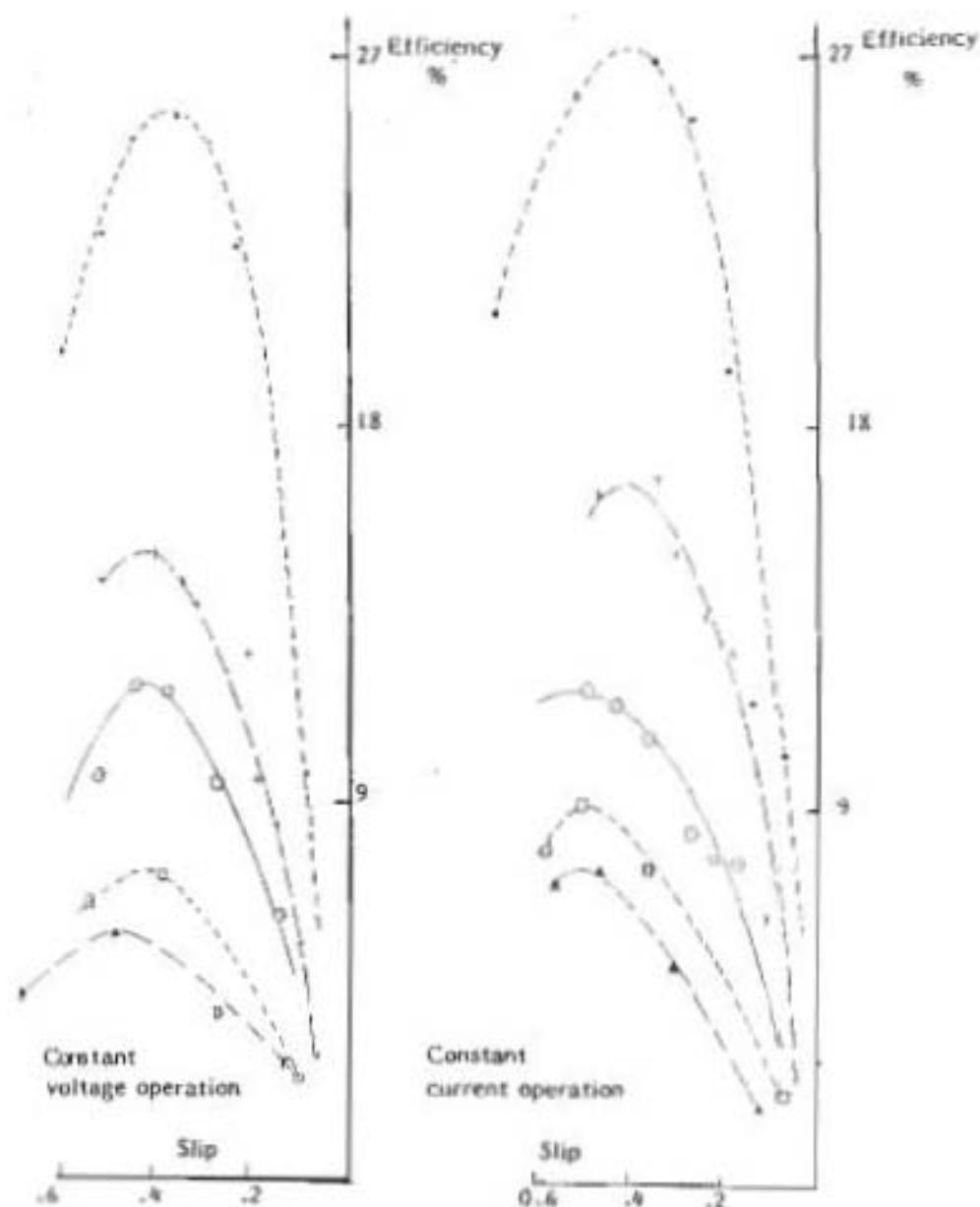


Fig. (2-e) : Measured flux - density - distribution for double sided excited stator with 120 electric degree phase shift.



- ▼-▼ Single sided-excited stator motor .
- ⊖-⊖ Single sided-excited stator backed by unexcited stator motor .
- x-x- Double sided-excited stator parallel connection motor .
- Double sided-excited stator cascaded connection with zero phase shift motor.
- Double sided-excited stator cascade connection with 120 electric degree phase shift m

Figure (3) : Measured thrust versus slip curves



- Single sided-excited stator motor.
- Single sided-excited stator backed by unexcited stator motor.
- ×-△-× Double sided-excited stator parallel connection motor.
- Double sided-excited stator cascaded connection with zero phase shift motor.
- ▽-▽-▽ Double sided-excited stator cascade connection with 120 electric degree phase shift motor.

Figure (4) : Measured efficiency-versus slip curves

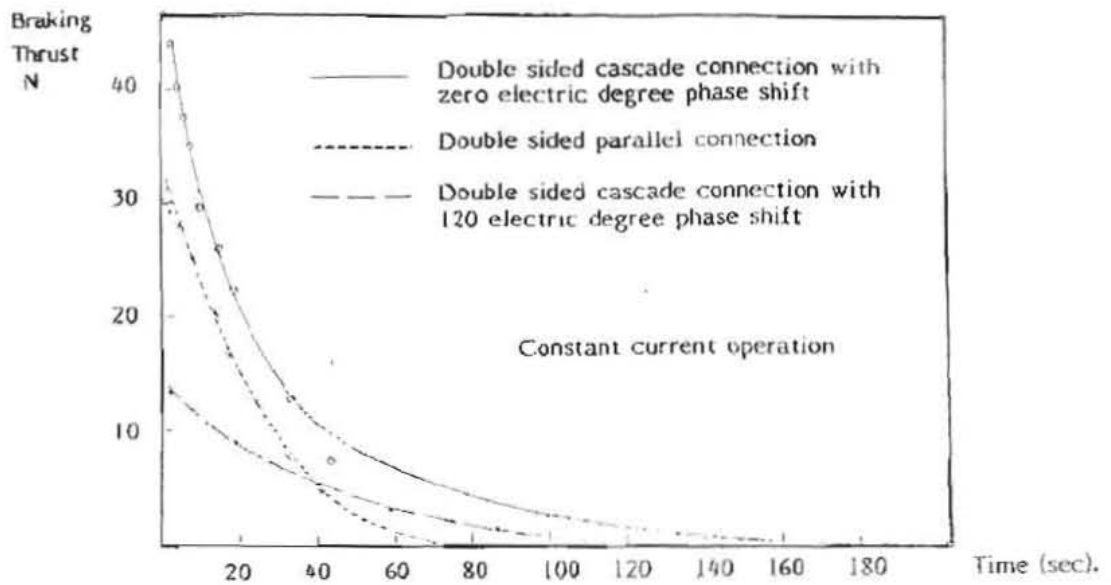


Fig. (5-a): Braking thrust versus braking time curves

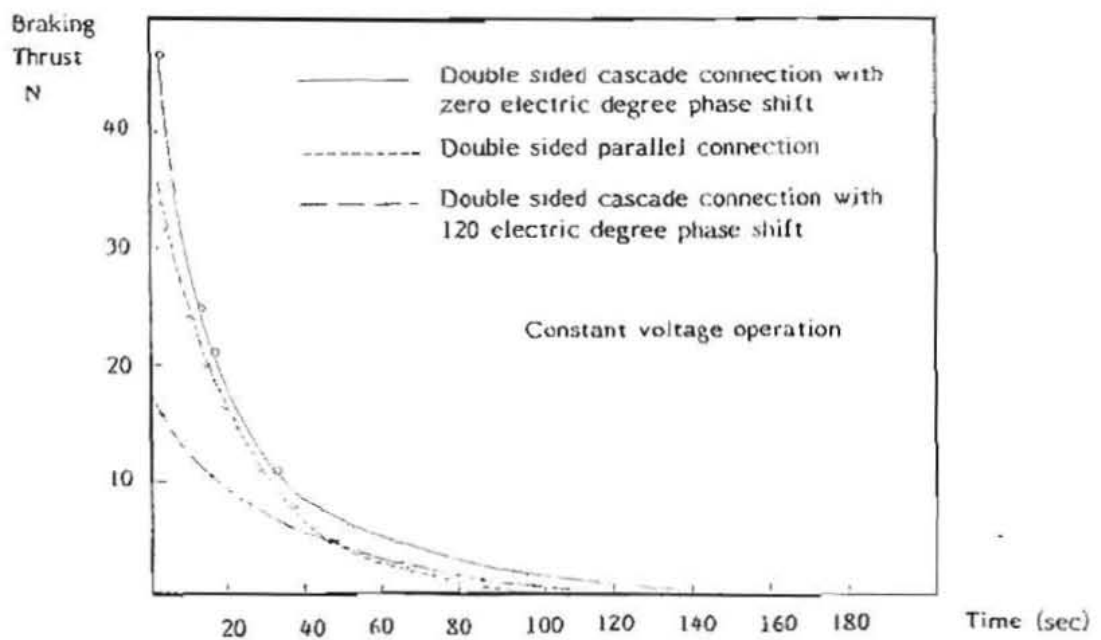
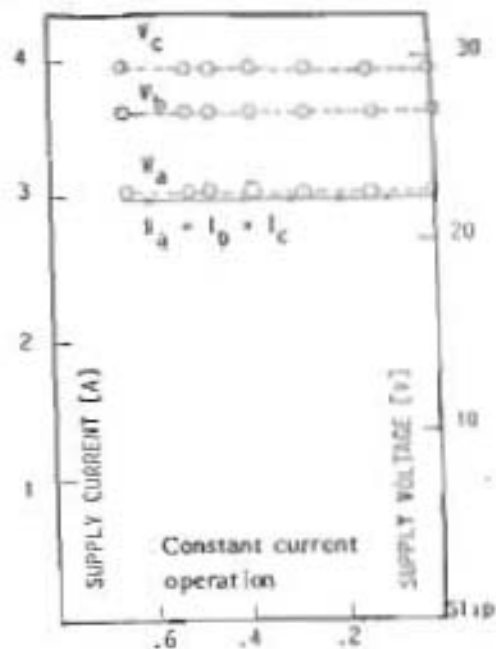
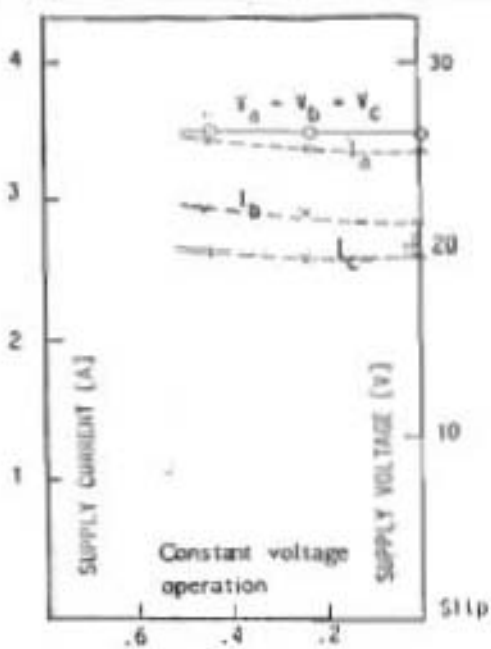


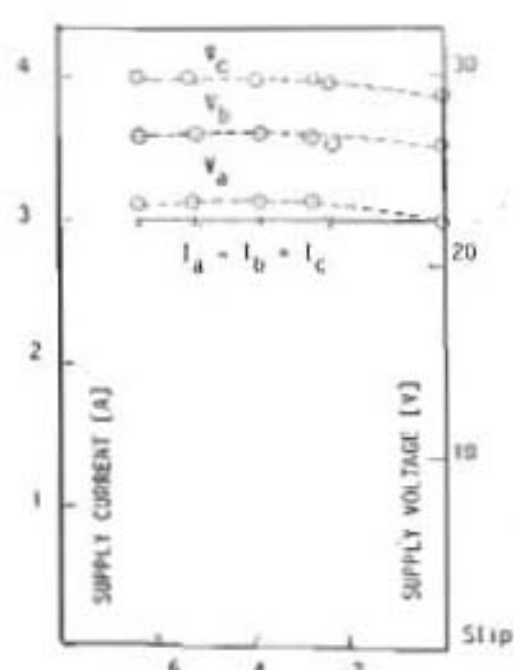
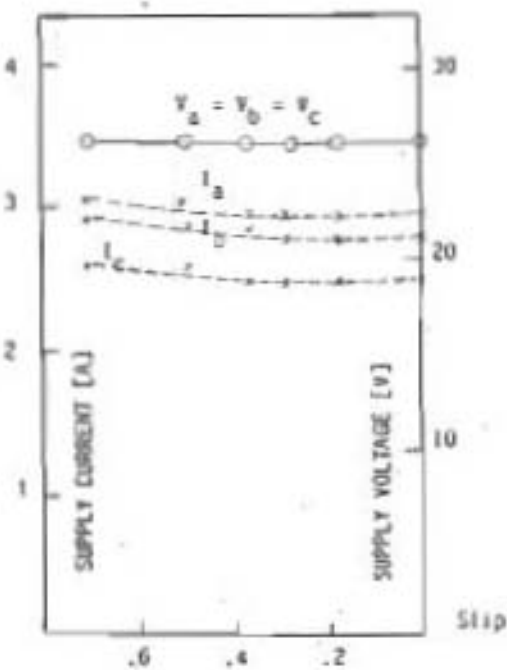
Fig. (5-b): Braking thrust versus braking time curves



Single sided excited stator LTM

Fig. (6-a): Measured supply current per phase per phase

Fig (7-a) : Measured supply voltage per phase



Single sided-excited stator backed by unexcited stator

Fig. (6-b) : Measured supply current per phase

Fig. (7-a) : Measured supply voltage per phase

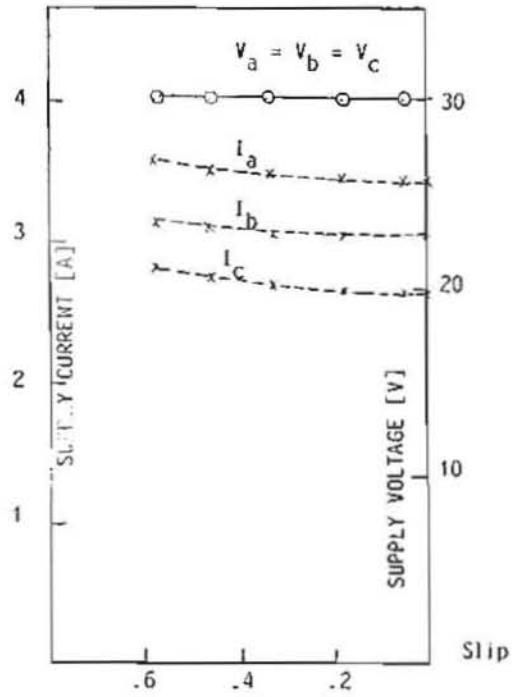


Fig (6-c) : Measured supply current per side (constant voltage operation)

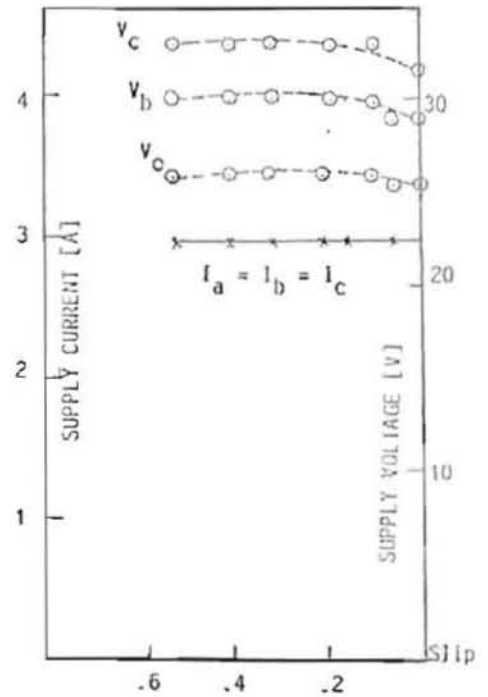
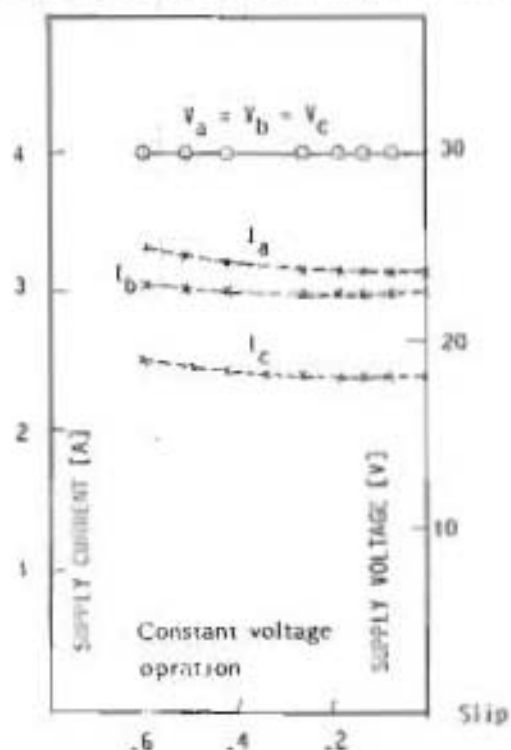


Fig (7-c) : Measured supply voltage per side (constant current operation)

double sided-excited stator parallel connection



Double sided-excited stator cascade connection with zero electric degree phase-shift

Fig. (6-d) : Measured supply current per phase

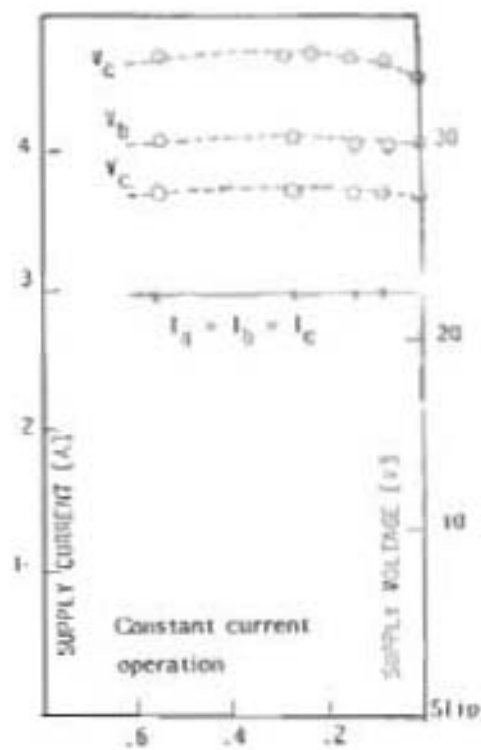
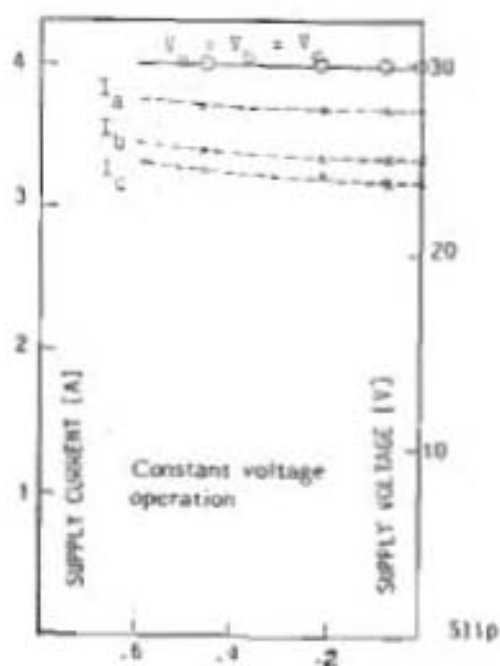


Fig. (7-d) : Measured supply voltage per phase



Double sided-excited stator cascade connection with 120 electric degree phase-shift

Fig. (6-e) : Measured supply current per phase

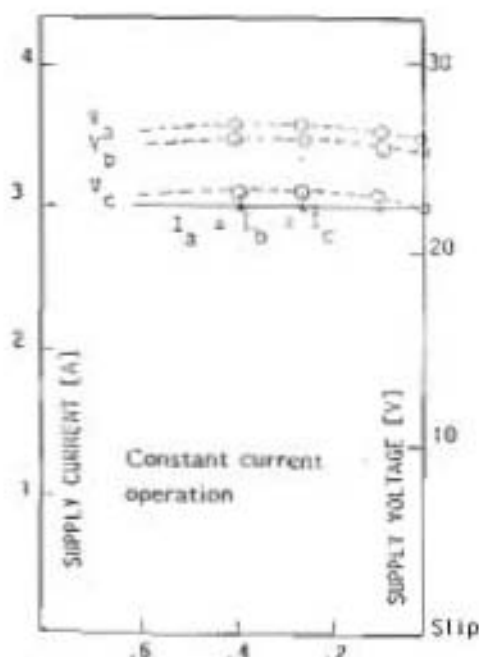


Fig. (7-e) : Measured supply voltage per phase